remote sensing

MDPI

Technical Note

Load Estimation Based Dynamic Access Protocol for Satellite Internet of Things

Mingchuan Yang *, Guanchang Xue, Botao Liu, Yupu Yang and Yanyong Su

Communication Research Center, Harbin Institute of Technology, Harbin 150001, China
* Correspondence: mcyang@hit.edu.cn

Abstract: In recent years, the Internet of Things (IoT) industry has become a research hotspot. With the advancement of satellite technology, the satellite Internet of Things is further developed along with a new generation of information technology and commercial markets. However, existing random access protocols cannot cope with the access of a large number of sensors and short burst transmissions. The current satellite Internet of Things application scenarios are divided into two categories, one has only sensor nodes and no sink nodes, and the other has sink nodes. A time-slot random access protocol based on Walsh code is proposed for the satellite Internet-of-Things scenario with sink nodes. In this paper, the load estimation algorithm is used to reduce the resource occupancy rate in the case of medium and low load, and a dynamic Walsh code slot random access protocol is proposed to select the appropriate Walsh code length and frame length h. The simulation results show that the slotted random access protocol based on Walsh code can effectively improve the throughput of the system under high load. The introduction of load estimation in the case of medium and low load can effectively reduce the resource utilization of the system, and ensure that the performance of the access protocol based on Walsh codes does not deteriorate. However, in the case of high load, a large resource overhead is still required to ensure the access performance of the system.

Keywords: satellite Internet of Things; random access protocol; load estimation; spread spectrum technology

Citation: Yang, M.; Xue, G.; Liu, B.; Yang, Y.; Su, Y. Load Estimation Based Dynamic Access Protocol for Satellite Internet of Things. *Remote Sens.* **2022**, *14*, 6402. https://doi.org/10.3390/rs14246402

Academic Editor: Johnson Ihyeh Agbinya

Received: 14 November 2022
Accepted: 16 December 2022
Published: 19 December 2022

1. Introduction

The Internet of Things (IoT) has become the third wave of the development of the information industry after computers and the Internet, but the deployment of IoT base stations on the ground will face many limitations [1]. As an extension of the satellite Internet, the satellite Internet of Things is further developed under the promotion of the new generation of information technology and commercial market [2]. In recent years, the cost of satellite launch and development has been continuously reduced. Many satellite communication companies are developing low-orbit IoT small satellite constellations to provide global users with low-cost, wide coverage, and low-latency IoT services. Traditional mobile and fixed satellite operators represented by Inmarsat, Iridium and Eutelsat have also deployed in this field in various ways to seek new business growth points [3].

Iridium Communications announced a partnership with Amazon Web Services (AWS) in 2018 to develop a satellite-based IoT application network called Cloud Connect [4]. Iridium Cloud Connect is the first satellite cloud-based solution to provide true global coverage for IoT applications. This new service from Iridium Communications combines Iridium IoT capabilities with AWS IoT and cloud services to expand customer IoT coverage to over 80% of the planet that lacks ground coverage [5]. The Orbcomm system is a commercial low-orbit satellite constellation for bidirectional short data transmission, but the user terminals of the Orbcomm system currently use low-cost VHF electronics. Due to the simple antenna, compact structure and low power consumption, the Orbcomm system can provide satellite IoT services. Currently, the Orbcomm satellite system can provide various

IoT services such as data collection services for remote transmission, monitoring services, tracking and positioning services, messaging and email [6]. The ARGOS system established by France and the United States uses low-orbit satellites as a carrier for transmitting various environmental monitoring data and positioning measurement instruments, providing good communication for hydrometeorological monitoring instruments in high latitudes. ARGOS deploys a satellite-tracking section drift buoy every 300 km in the global ocean, forming a huge global ocean real-time observation network through 3000 buoys. The ARGOS system can be applied to climate change monitoring, oceanographic and meteorological monitoring, conservation, water resource monitoring, and marine resource management and biodiversity conservation [7].

Ref. [8] proposes a satellite IoT system architecture for low-energy end-users. The system relies on the low earth orbit (LEO) constellation and the Contention Resolution Diversity Slotted ALOHA (CRDSA) protocol, which verifies that the LEO satellite can meet the requirements of the satellite Internet of Things system under the CRDSA protocol. However, GEO satellites need to reduce the cost and complexity of nodes, making GEO satellites an important scenario for CRDSA and receiver SIC algorithms. In addition, CRDSA++ has made certain modifications on the basis of CRDSA, which can support more than two packet copies [9]. Ref. [10] proposed the Sliding Window Contention Resolution Diversity Slotted ALOHA (SW-CRDSA) protocol. Moreover, SW-CRDSA replaces frames with sliding windows, thereby reducing the requirement of frame synchronization for the entire system. A slotted access system requires terminals to keep time slot synchronization, but the synchronization overhead will greatly reduce the system efficiency, which is not conducive to low-cost terminal solutions. Therefore, the literature [11] proposed the Spread Spectrum ALOHA (SSA) scheme working in asynchronous mode. Under the conditions of using equal power multiple access, high-performance physical layer forward error correction coding (such as coding rate ≤ 0.5) and low-order modulation (such as BPSK, QPSK), the SSA scheme can be used for the same packet loss rate (PLR) can achieve higher throughput. However, the SSA scheme is sensitive to the power imbalance of multiple access carriers, which will seriously affect the throughput of the SSA scheme.

Ref. [12] proposes a hybrid access protocol that satisfies the DVB-RCS2 standard. The terminal can have three different working modes in the superframe, namely pure RA access, pure DA access, and Random Access (RA) and Dedicated Access (DA) hybrid access. When the remaining space of the medium access control (MAC) layer queue of the terminal is sufficient, access is always performed according to the RA protocol. When the remaining space exceeds a certain threshold, DA mode is introduced to obtain more throughput. However, hybrid access protocols are more complex to implement and are typically used for return channel satellite ground terminals (RCSTs) rather than resource-constrained small sensors. Ref. [13] proposed the application scenario of satellite IoT with sink nodes in the smart grid. Ref. [14] proposed the application scenario of satellite communication in the ground sensor network. In addition, the literature [15] presents a throughput estimation model for satellite IoT with sink nodes. The access protocols used in the scenario are mainly complex access protocols such as CRDSA protocol and IRSA protocol, making full use of the sufficient energy provided by the sink node to reduce the computational pressure of each sensor node. Due to the aggregation function of the aggregation node for user terminal data and the higher performance of the aggregation node than that of the user terminal, an access protocol with higher complexity can be used. Moreover, in the satellite IoT scenario with aggregation nodes, a certain access overhead can be tolerated.

At present, the RA protocol in the MAC layer competition access protocol has low overhead, low power consumption, and short access delay, and is very suitable for applications in the satellite Internet of Things scenario. However, the throughput performance of access protocols is mostly better under low and medium load conditions, and the performance will drop sharply when the load is too high. On the other hand, the throughput performance of the DA protocol under high load conditions is much better than that of the random access protocol. However, the larger distance between the satellite and the ground leads to a

higher round-trip delay, which makes it difficult to meet the service requirements that have strict delay requirements. Although the hybrid access protocol can ensure a small access delay and improve the total throughput of the system, the implementation complexity of the algorithm is high. For terminals with limited power and lower cost requirements, the current hybrid access method is not suitable. For satellite IoT scenarios with sink nodes, this paper follows the time-slotting method in the CRDSA protocol, and introduces a spreading code sequence with orthogonal characteristics to further distinguish users.

The rest of this paper is organized as follows: Section 2 describes the architecture of satellite Internet of things. Section 3 analyzes satellite IoT scenarios with sink nodes. Section 4 presents simulation results for metrics such as throughput and packet loss rate performance. Section 5 is the conclusion of this paper.

2. The Architecture of Satellite IoT

According to the research status of satellite IoT, there are mainly two application scenarios of satellite IoT, namely, scenarios of satellite IoT with sink nodes and scenarios of satellite IoT without sink nodes. The following part of this paper studies the scenarios of satellite IoT with and without sink nodes, respectively, gives the commonly used random access protocols in different scenarios and analyzes the performance. The scenarios of satellite IoT are mainly divided into two categories: one is the scenario of IoT with sink nodes, which is mainly applied to the network in land areas such as urban areas and forest areas; The other is the IoT scenario where there are no sink nodes but only sensor nodes, mainly to deal with the areas where it is difficult to establish sink nodes, such as oceans and deserts. Figures 1 and 2 show satellite IoT scenarios with sink nodes and satellite IoT scenarios without sink nodes, respectively. The existence of sink nodes makes the two scenarios have certain differences in access mode requirements:

(1) Restriction of access complexity: Since the energy supply of sink nodes is sufficient, the access mode with higher complexity can be selected.
(2) Limitation of satellite height: the low energy characteristics of sensor nodes determine that their transmitting power is limited. In order to successfully access the satellite, the distance between the sensor and the satellite needs to be reduced, so the satellite height is limited to a certain extent.
(3) Limitation of application environment: the establishment of sink nodes requires certain environmental support, and it is difficult to place enough sink nodes in deserts, oceans and other areas that are difficult for human beings to reach.

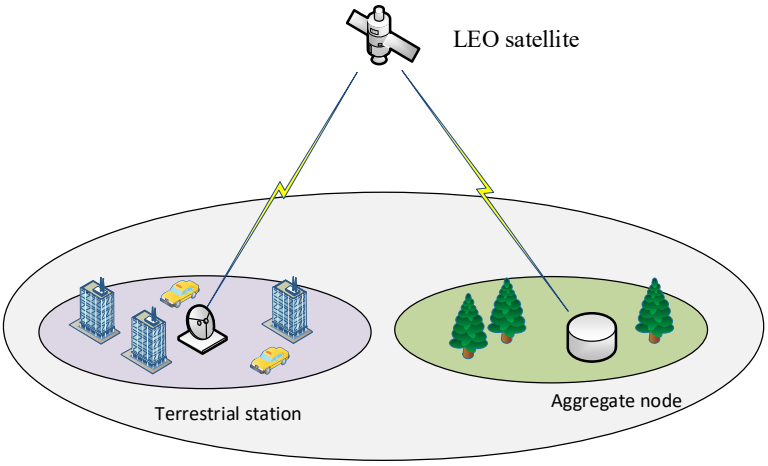

Figure 1. Satellite IoT scenario model with sink nodes.

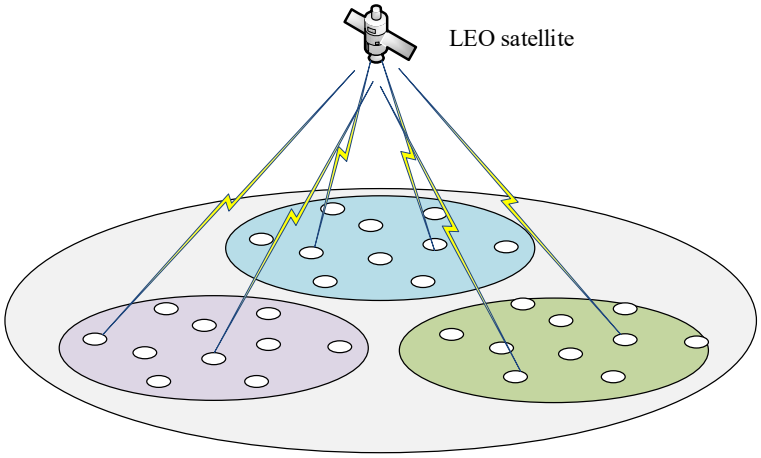

Figure 2. Satellite IoT scenario model without sink nodes.

2.1. Satellite Iot Scenarios without Sink Nodes

2.1.1. ALOHA Protocol

In a network containing multiple-user terminals, as long as the user terminal has a packet that needs to be sent, the packet will be sent immediately; if a collision occurs, the user terminal will retransmit the packet after a random retreat for a period of time. Its working principle is shown in Figure 3. The advantage of pure ALOHA protocol is that its implementation is very simple, and it can always support heterogeneous information packets of different lengths, so it is very suitable for satellite IoT, which is a network where terminals work suddenly [16,17]. But the pure ALOHA protocol also has a big problem, that is, its maximum normalized throughput is too low, only 0.184. Its low throughput performance is mainly caused by the generation of "collisions" and new "collisions" caused by packet retransmission. Especially in the case of excessive load, the existence of "collision" almost makes the system unable to work, resulting in the instability of the system [18,19].

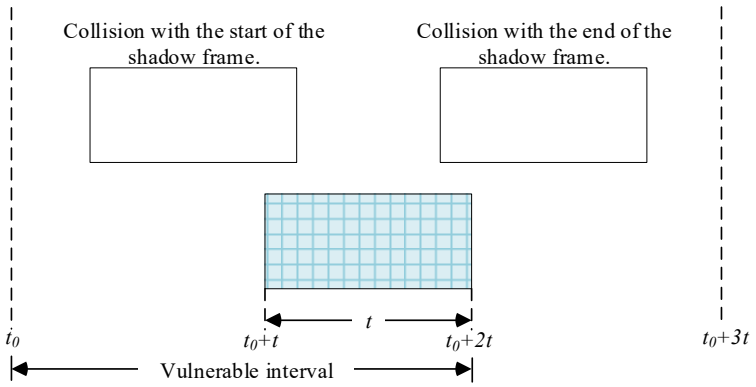

Figure 3. The working principle of pure ALOHA.

In a scenario without an aggregate node, the data packets transmitted by a single node are very small, so time synchronization or resource application operations will greatly increase overhead, causing a sharp drop in transmission efficiency. Therefore, the ALOHA protocol, which is asynchronous and does not need to apply for resources, is suitable for the application scenario of the satellite Internet of Things, but it needs to solve the problem of low throughput performance.

2.1.2. SA Protocol

The SA protocol divides the time axis into several time slots, and all nodes can only send packets at the beginning of the time slot, requiring all time slots to be synchronized.

As shown in Figure 4, the size of the time slot is equal to the transmission time of a packet. Under the SA protocol, because the time slots of all terminals are synchronized, there are only two states: complete non-collision and complete collision [20–23].

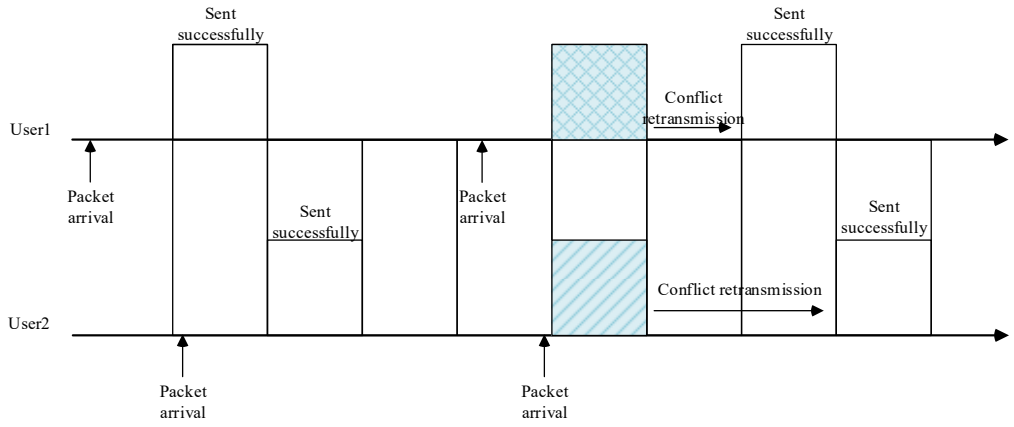

Figure 4. The working principle of slotted ALOHA.

2.2. Satellite Iot Scenarios with Sink Nodes

The scene in which sink nodes can be established is mainly used in urban areas, forest areas, suburbs and other ground areas. The single-star access scenario is shown in Figure 2. Due to the existence of sink nodes, there is no clear requirement for satellite height. Due to the aggregation effect of the sink node on the user terminal data and the higher performance of the sink node than the user terminal, the higher complexity access protocol can be used in the satellite IoT scenario with sink node. It can also tolerate a certain amount of access overhead. The access protocols used in these scenarios are mainly high complexity access protocols such as CRDSA protocol and IRSA protocol, which make full use of the sufficient energy provided by the sink node to reduce the computing pressure of each sensor node.

2.2.1. CRDSA Protocol

CRDSA protocol allows the user to generate two copies of the packet, randomly placed in two slots within a MAC frame, as shown in Figure 5. In the Figure 5, there is only one Burst PK3 in Slot 5, and more than one in the rest. Thus, PK3 can be properly received and decoded. According to the PK3 obtained in Slot 5, another PK3 in Slot 4 can restore the signal of PK2 based on the signal of PK3 and the signal received in Slot 4. After the obtained PK2, the interference between PK1 and PK2 in Slot1 can be eliminated, and PK1 can be obtained, and so on, until it can no longer be eliminated. Burst that cannot be restored is retransmitted. This process is called Successive Interference Cancellation (SIC). The SIC process leads to the restoration of many packets that were originally discarded due to conflicts, thus avoiding retransmission and thus greatly improving throughput and delay [24–26].

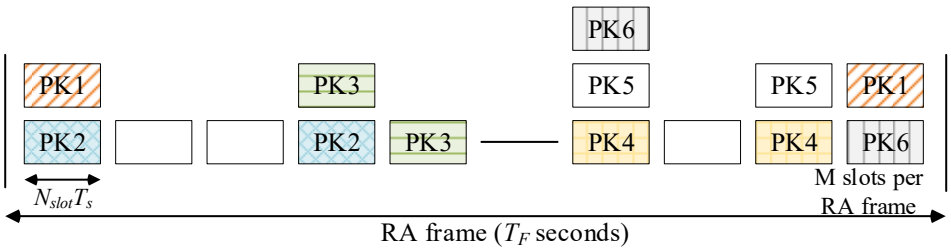

Figure 5. The working principle of CRDSA.

2.2.2. IRSA Protocol

IRSA protocol is improved on the basis of CRDSA protocol. In the CRDSA protocol, each packet sends two copies in one frame. In IRSA, each packet no longer sends a fixed number of 2 copies, but sends a random number of copies according to a probability distribution. By optimizing the probability distribution function, the optimal performance can be obtained. Under medium and low load conditions, IRSA protocol has a significant performance improvement compared to CRDSA protocol. However, under high load conditions, the performance of IRSA protocol decreases significantly, and the packet loss rate increases sharply. Therefore, the benefits of the IRSA protocol can only be seen in the medium to low load networks. However, the CRDSA and IRSA protocols have an obvious performance problem, that is, when the number of users exceeds the number of time slots, the performance drops dramatically. This is mainly because both CRDSA and IRSA protocols use SIC to solve the problem of multi-user access interference. However, in the case of high load, the increase in the number of "loops" greatly affects the performance of SIC to solve packet conflicts, and even an increase in the number of iterations does little to improve performance. This paper proposes an effective access scheme for satellite IoT scenarios with sink nodes.

3. Dynamic Satellite IoT Access Protocol Based on Load Estimation Algorithm

3.1. Slot Random Access Protocol Based on WALSH Code

This paper considers the reverse link in the satellite IoT, where the sink node is used as the terminal of the network to access the LEO satellite. Each sink node has a spreading code encoding and decoding function, and the codebook used by it will be broadcast to each sink node by LEO satellite. In order to simplify the system model, all sink nodes modulate the data on the same frequency. In addition, the channels experienced by all data packets are Gaussian white noise channels, and there is no unbalanced data packet power.

Assume that all user traffic obeys the Poisson distribution with the parameter GTs. Where G represents the normalized load of the network, and T_s represents the duration of the time slot, the probability density function of the data packet arriving at the satellite can be expressed as:

$$\rho(k) = \frac{(GT_s)^k}{k!} e^{-(GT_s)} \tag{1}$$

In this scenario, all user packets have a fixed duration of T seconds and each packet is L bits long. In each slot there are:

$$T_s = T + \tau_{aw} \tag{2}$$

where τ_{aw} represents the length of time from the start of a time slot to the opening of the access window (AW). Because of the orthogonal properties of Walsh codes themselves [27], conflicting packets in a slot can be separated without the need for the SIC algorithm in CRDSA. Therefore, in the time slot random access protocol based on Walsh code, each user only needs to send one packet in one frame. The slot random access protocol based on Walsh code is described in detail in the following sections.

3.1.1. Codebook Design

Given that the total number of users N_u, $\mathcal{D} = \{\mathbf{e}_1, \mathbf{e}_2, \ldots, \mathbf{e}_{N_c}\}$ represents N_c available Walsh code sequences, the Walsh code sequence used by the k-th user is:

$$\mathbf{s}_k = \mathbf{e}_{\mathrm{mod}(k,N_c)+1} \tag{3}$$

Then, the codebook $C = \{\mathbf{s}_1, \mathbf{s}_2, \ldots, \mathbf{s}_{N_u}\}$ will eventually be sent by the satellite to all users.

3.1.2. Conflict Resolution Algorithm

When a user sends data, it is very likely that multiple data will be sent in the same time slot, so it is necessary to solve the conflicting data packets at the receiving end, so as to obtain complete user information. The specific conflict resolution algorithm flow is shown in Figure 6. When the satellite receiver receives the data, the receiver will store the data in the satellite register by frame. When conflict resolution is carried out, the data of the first time slot in a frame is read first, and the cross-correlation operation is carried out between the data and all the sequences in the codebook. If the cross-correlation value is higher than the set threshold value in the process of operation, it is determined that there is a solvable data packet, and the data is despreaded and reconstructed. After the reconstruction is completed, the reconstructed data is deleted from the current time slot, and the correlation operation of the sequence continues until there is no more correlation value greater than the threshold value, which means that all the data that can be settled in the current time slot has been extracted. At this point, the data of the next time slot is read, and so on.

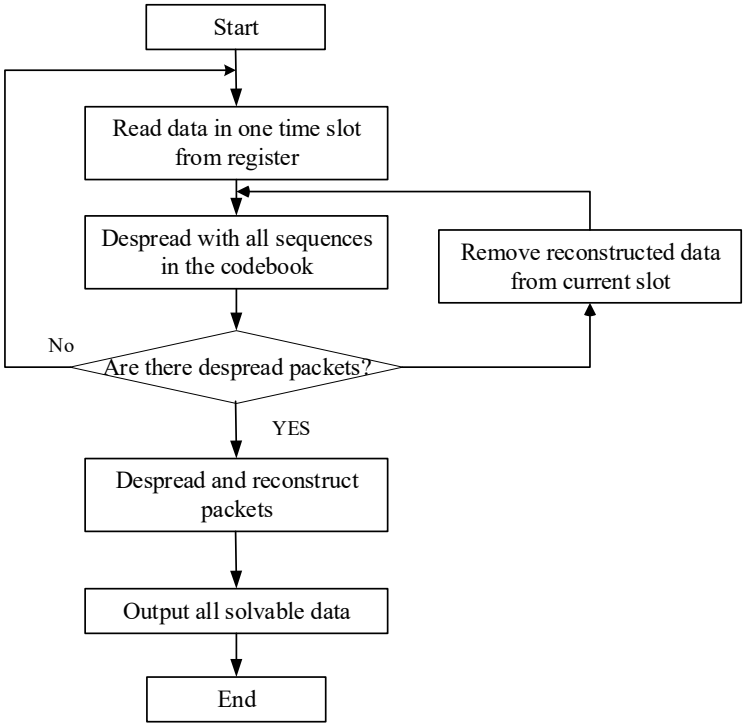

Figure 6. Flowchart of the conflict resolution algorithm.

The advantage of this conflict resolution algorithm is that users only need to send one packet in a frame, that is, abandoning the mechanism that requires duplicate data packets in CRDSA, which greatly improves the transmission efficiency. In addition, for a single time slot, as long as the user uses different Walsh code sequences, two or more data packets can be solved in one time slot. Compared with only one data packet in one time slot in CRDSA, the maximum number of users that can be accessed in one frame is increased based on the Walsh code sequence.

3.1.3. Capacity Upper Bound of Random Access Protocol Based on Walsh Code

Walsh code is a pseudo-noise code, and its upper bound on capacity is directly related to the signal to interference and noise ratio (SINR) and its processing gain. For Walsh code sequences, there are:

$$G_p \approx N_c \tag{4}$$

where G_p is the processing gain of the system after using Walsh code. The multiple access interference power of one user received by the satellite is given in the Equation (5):

$$P_{\mathrm{MAI}} = (M-1)\frac{P}{G_p} = N_0 R_b \tag{5}$$

Equation (5) can obtain the maximum number of simultaneous user packets in a single time slot. Therefore, when the Walsh code-based time slot random access protocol is applied, the total number of users theoretically accessible to the system M_{max} can be given by Equation (6):

$$M_{\max} = N_{\mathrm{slots}} M = N_{\mathrm{slots}} \left(\frac{G_p}{(E_b/N_0)} + 1 \right) \tag{6}$$

where N_{slots} represents the number of time slots in a frame and the quality factor of the on-board demodulator. From Equation (6), it can be seen that the total number of users accessible to the system is directly related to the number of time slots in a frame, the processing gains of spread spectrum sequence and the quality factor of the demodulator. Therefore, to increase the total number of users that can be accessed in the system, the processing gain of the spread spectrum code and the number of time slots of a frame can be increased, respectively.

3.2. Load Estimation Algorithm

According to the research of different random access protocols mentioned above, it can be seen that different protocols perform differently under different load conditions. In order to select the appropriate access protocol according to the load condition, the load estimation algorithm is necessary.

Firstly, the scene model of the satellite wireless network system is given. Let n represent the size of the collision set to be estimated, and ω represent the current frame length, that is, the number of time slots contained in a frame. Each slot can have three states: idle state (Idle), successful access state (Successful) and collision state (Collided) [28], indicating that the number of packets in the slot is 0, 1, and greater than 1, respectively. Then, the expected number of slots in each state in a frame is:

$$m_C(n) = \omega \left[1 - \frac{n}{\omega} \left(1 - \frac{1}{\omega} \right)^{n-1} - \left(1 - \frac{1}{\omega} \right)^{n} \right] \tag{7}$$

$$m_S(n) = \omega \left(1 - \frac{1}{\omega} \right)^{n-1} \tag{8}$$

$$m_I(n) = \omega \left(1 - \frac{1}{\omega} \right)^{n}. \tag{9}$$

Therefore, through observation, the number of time slots in three different states in a frame can be obtained, represented by vectors, and the estimated value of n can be obtained. In this paper, a maximum likelihood estimation algorithm (MLE) is presented. The traditional MLE algorithm uses Equation (10) to estimate the collision set size n.

$$\mathcal{H}_{\mathrm{MLE}}(\mathbf{v}) = \mathrm{argmax} P_n(\mathbf{v}) \tag{10}$$

Among them,

$$P_n(\mathbf{v}) = \binom{\omega}{s} \binom{\omega - s}{c} \sum_{j=0}^{c} \sum_{l=0}^{c-j} \binom{c}{j} \binom{c-j}{l} \frac{(-1)^{c-j} n! j^{n-l-s}}{\omega^n (n-l-s)!} \tag{11}$$

According to the assumption of the IoT system in this section, that is, the arrival process of data packets obeys Poisson distribution and is independent of each other, and

the parameter $\mu = n/\omega$ of this distribution is unknown. Under this assumption, we can get [29–31]:

$$\hat{P}_n(\mathbf{v}) = \mu^s e^{-\mu\omega}(e^{\mu} - 1 - \mu)^c \tag{12}$$

$$\mathcal{H}_3(\mathbf{v}) = \lceil \omega\hat{\mu} \rfloor \tag{13}$$

According to the Equation (10), the derivative of the Equation (12) and making it equal to 0, the estimated value of the parameter, that is, the solution of the Equation (14) can be obtained. The estimated value of n can be obtained after substituting Equation (13).

$$\frac{\mu\omega - s}{c} = \frac{\mu(e^{\mu} - 1)}{(e^{\mu} - 1 - \mu)} \tag{14}$$

3.3. Dynamic WALSH Code Time Slot Random Access Protocol Based on Load Estimation Algorithm

In order to save resources as much as possible on the basis of meeting certain throughput requirements, the load estimation algorithm is essential. In this system, the load estimation will be completed by the onboard load, and the estimated results will be broadcast by the satellite to all registered users to adjust the codebook and frame length used by the users.

The architecture of the client side and the on-board payload are shown in Figures 7 and 8. After the MAC packet segment is generated by the user's data, according to the frame length and codebook information in the instructions broadcast by the satellite, the packet segment is spread spectrum operation, and enters the cache, and the appropriate time slot is selected to send. When the satellite receives the demodulation data, it firstly caches the data by frame, and then the correlator carries out the relevant operation on the data by time slot. If there is any data packet that can be solved, it will be unexpanded, and the data packet will be reconstructed while decoding the output. The reconstructed data packet will be deleted from the cache data of the current time slot, and relevant operations will continue in the next step. At the same time, the load estimation module also reads the data of a frame from the cache, counts the number of time slots in different states, and completes the load estimation. The appropriate frame length and codebook are selected according to the estimated results, and the corresponding information is broadcast to each user. The workflow of the load estimation module is described in detail below:

1. set the load threshold before using it for the first time.
2. read the data from the cache and get the load estimate according to the time slot state statistics in a frame of data.
3. the appropriate frame length and codebook information are selected according to the comparison between the load estimate and the load threshold.

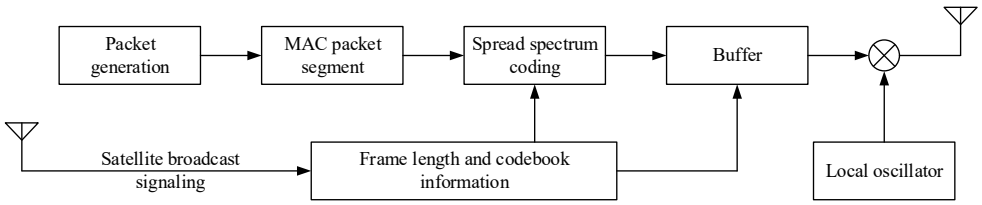

Figure 7. User-side architecture design.

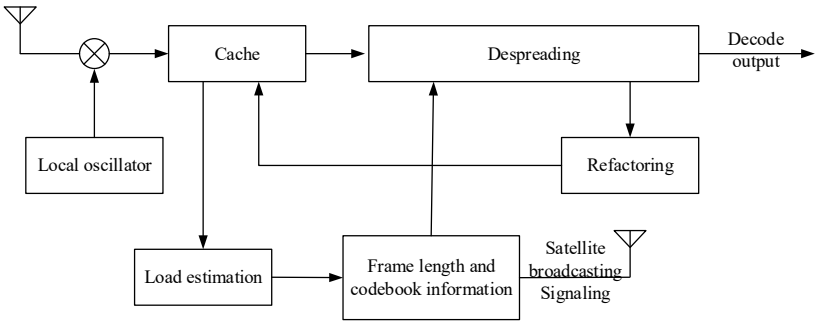

Figure 8. On-board load architecture design.

It should be noted that, due to the processing delay of the onboard load correlator and the propagation delay between the satellite and the ground, the setting of the load threshold needs to have a certain margin. The number of margin users for the threshold is set to 5 in the simulation. Two load thresholds are set in the system simulation, and there are 3 different combinations of frame length and codebook. When the frame length and the selected codebook reach a certain threshold, the frame length and the selected codebook will not change at the same time, thereby reducing the complexity of switching. This section assumes that the system requires a packet loss rate of no less than 10^{-1}. The load threshold is set as follows: When the estimated load value is lower than 105, the number of time slots is 50, and the Walsh code family of order $r = 5$; When the load estimate is between 105 and 175: the family of Walsh codes with 50 time slots and order $r = 6$. When the estimated load value is greater than 175, the Walsh code family with 100 time slots and order $r = 6$ is selected.

4. Simulation and Analysis

4.1. Simulation and Analysis of Time Slot Random Access Protocol Based on WALSH Code

In this simulation, the CRDSA protocol performance data of sending two copies of packets is used as a comparison reference. In order to better reflect the performance of random slot access protocol based on Walsh code, the throughput and packet loss rate energy curves of Walsh code sequences with order $r = 5$ and $r = 7$ at slot number $N_{\text{slots}} = 50$ are simulated, respectively. Comparison curve of access performance is shown in Figure 9. For the slot random access protocol based on Walsh code, due to the orthogonality of Walsh code, when the number of users exceeds the number of slots, a higher number of access can also be guaranteed. However, this access protocol still has a capacity upper bound, so when the number of users reaches a certain value, the number of users in the system will be very limited.

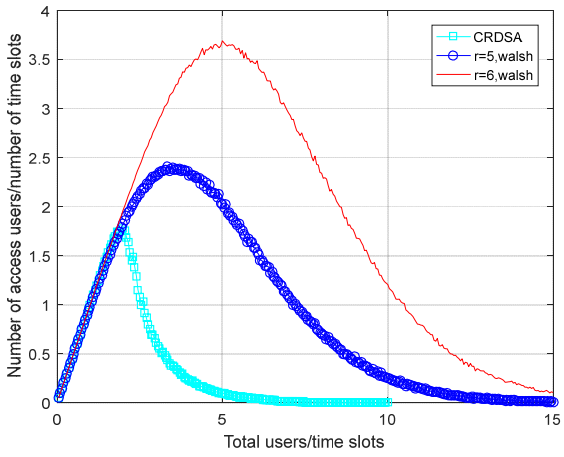

Figure 9. Throughput comparison curve under the same number of time slots.

Figure 10 shows the packet loss rate energy curve under this condition, which can further verify the performance differences of three different access modes. As can be seen from the figure, the CRDSA protocol performs better under low load conditions because it is almost impossible to "loop" under low load conditions, but the reuse of Walsh codes affects the performance of Walsh codes. However, under the condition of high load, the performance of CRDSA protocol has obvious and sharp decline, at which time the advantages of Walsh code can be reflected. The performance of random slot access protocol based on Walsh code is improved with the increase of order R of shift register of the code sequence. The performance characteristics of Walsh code-based slot access protocols with a different number of slots and different orders will be analyzed in detail in the following sections. Figure 11 shows the throughput performance curves when using the Walsh sequences at $r = 5$ and $r = 7$ in frames with 50 and 100 slots, respectively.

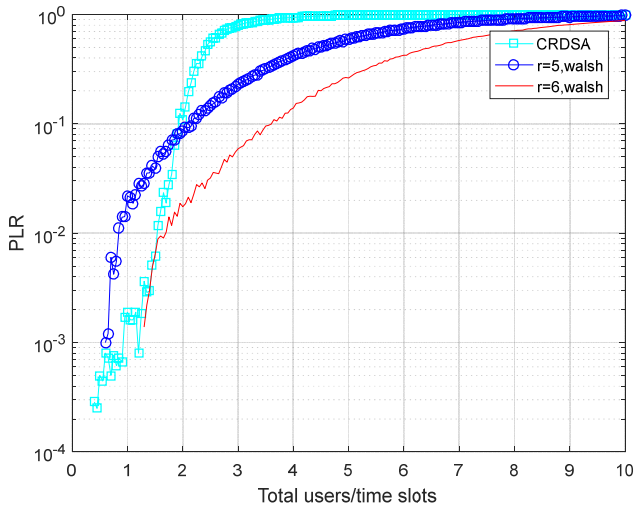

Figure 10. Comparison curve of PLR under the same number of time slots.

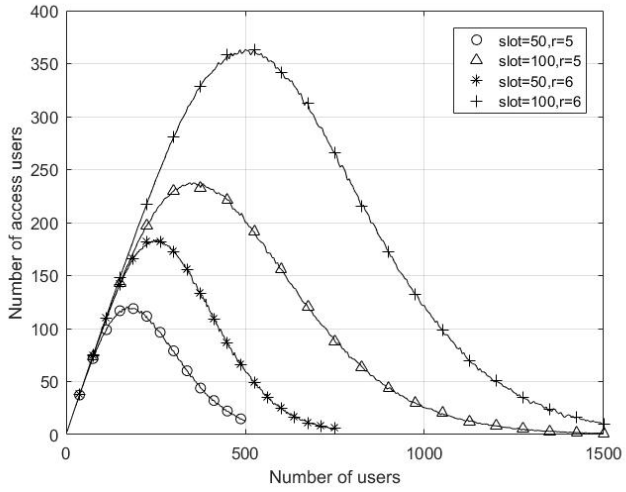

Figure 11. Throughput performance curve of Walsh code time slot random access protocol with different parameters.

The simulation results show that the increase of frame length can further improve the throughput performance of the system. Because for the same number of users, the more time slots a frame contains, the fewer conflicting packets in a single time slot. According to Equation (6), increasing the number of time slots in the frame can directly increase the upper bound of the user capacity of the system. The dotted line in the figure still represents the

ideal reference value for successful access for all users. As can be seen from Figure 11, when the number of users is less than 50, almost 100% access can be guaranteed by four different access modes. When the number of users increased to 100, a more obvious performance differences appeared: the number of time slots for 50 two-access modes, the current number of users reached twice the number of time slots and a certain performance degradation resulted, and for where the access time slot number is 100, the current number of users is no more than 2. Therefore, throughput performance reflected a certain advantage. When the number of users increased to more than 150, the number of time slots for 50 both access a significant performance deterioration. For using the Walsh code sequence of $r = 5$, the number of time slots for 100 access, the number of Walsh code sequence limits also led to the decrease of the throughput performance, the only time slot number and order number are all too high-access to continue to guarantee throughput.

The packet loss rate energy curve shown in Figure 12 more directly reflects the performance under four different access modes. In the actual system, there are always certain requirements for the packet loss rate of the system. If the packet loss rate of the system is required to be less than 10^{-2}, the maximum number of users that can be provided by the four access modes is 41, 65, 88 and 130, respectively. If the required packet loss rate of the system is less than 10^{-1}, the maximum number of access users that can be provided is 105, 175, 200 and 350. Although it can be seen from the simulation results that the higher the number of time slots in a frame and the higher the order of shift register of Walsh sequence, the better the access performance of this protocol, but at the same time, the higher the overhead. Therefore, in order to make use of the advantages of this protocol effectively, the load estimation algorithm is introduced here to further improve this protocol.

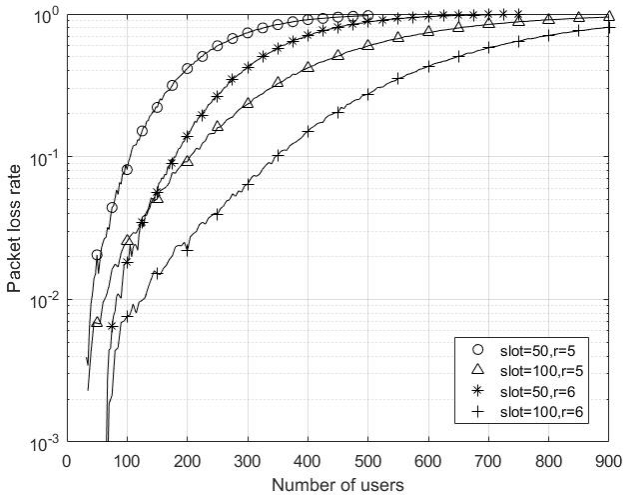

Figure 12. PLR performance curve of Walsh code timeslot random access protocol with different parameters.

4.2. Simulation and Analysis of Dynamic WALSH Code Slot Random Access Protocol Based on Load Estimation Algorithm

According to the assumptions and parameter settings mentioned above, the performance of the dynamic Walsh code random access protocol based on the load estimation algorithm is simulated. Its throughput performance and packet loss rate performance are shown in Figures 13 and 14. As can be seen from the figure, thanks to the load estimation, the protocol realizes the dynamic switching of frame length and codebook, and meets the corresponding throughput and packet loss rate requirements in different load ranges. However, it should also be noted that due to the existence of load estimation error, there is an obvious jitter problem in the performance of throughput and packet loss rate near the load threshold, in which when the load value reaches about 200 users, the jitter range of the packet loss rate is the largest.

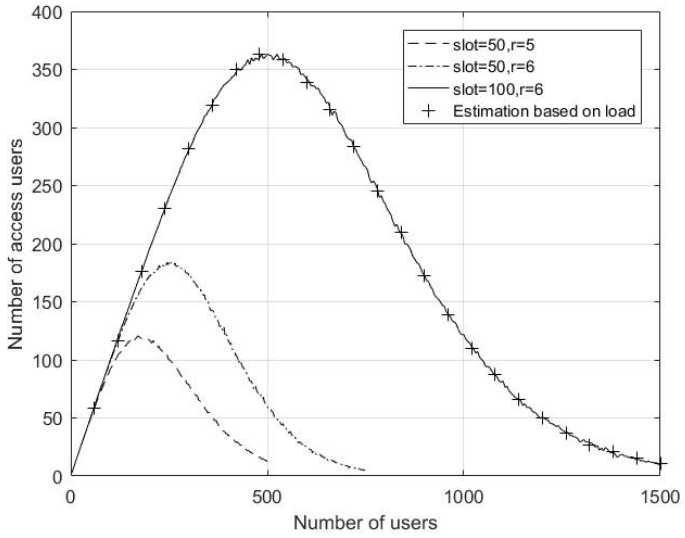

Figure 13. Throughput performance simulation curve of the improved protocol.

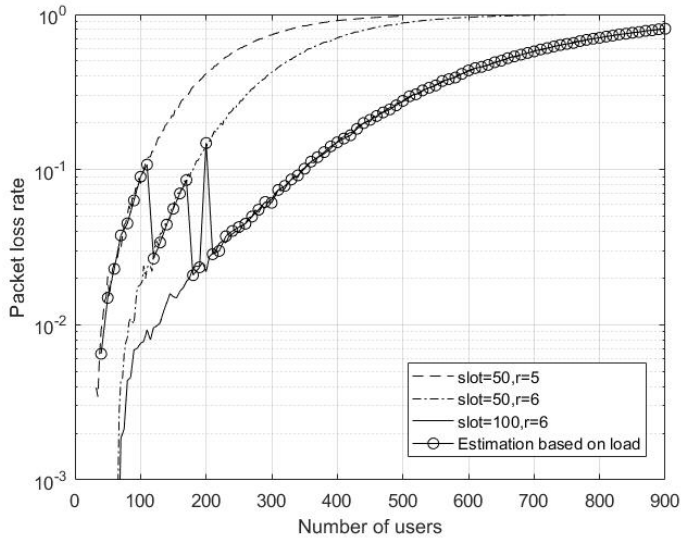

Figure 14. Simulation curve of packet loss rate performance of improved protocol.

In addition, in order to more intuitively see the saving effect of the load estimation algorithm on bandwidth and time resources, according to the hypothesis and definition of the system, the code length of Walsh code is directly related to the resource cost, while the frame length can be represented by the number of time slots in a frame. Here, it is defined as the resource occupancy rate, which can be calculated by Equation (15).

$$\beta = \frac{1}{2} \cdot \left(\frac{N_c}{N_{c\max}} + \frac{N_{\text{slot}}}{N_{\text{slotmax}}} \right) \tag{15}$$

Figure 15 shows the simulation curve of system resource usage. It can be seen from the figure that the dynamic Walsh code slot random access protocol based on load estimation occupies fewer resources in the case of low and medium load, and it only needs short spread spectrum code length and frame length to ensure access. However, with the increase of network load, the collision probability of user access increases. Only by increasing the length of spread spectrum code can the number of user access in a single time slot be increased, while increasing the frame length can reduce the probability of user conflict in a single time slot. Therefore, more resources will be occupied in the case of high

load. Therefore, the introduction of the load estimation algorithm can reduce the resource overhead under medium and low load conditions, but it still needs to pay a large overhead to ensure access under high load.

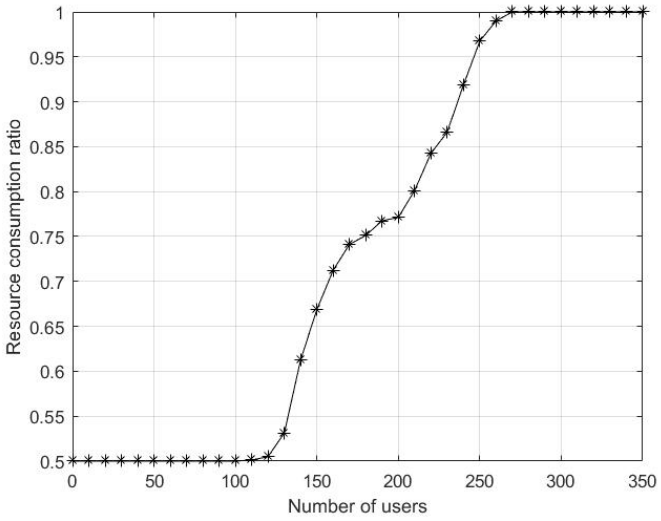

Figure 15. Resource occupancy of dynamic Walsh code slot random access protocol.

5. Conclusions

This paper mainly studies the satellite Internet of Things scenario with sink nodes. Through the analysis of the CRDSA protocol, a time slot random access protocol based on Walsh code is proposed to solve the problems existing in the CRDSA protocol. The protocol breaks the limitation that only one user data packet can be correctly received in a time slot, greatly increases the number of accessible users in a frame, and at the same time enables the protocol to achieve high performance without relying on repeated data packets. However, the application of Walsh codes also brings some overhead, which reduces the throughput performance of the system. In order to reduce the overhead as much as possible, a dynamic Walsh code slot random access protocol based on the load estimation algorithm is proposed. The load estimation algorithm is used to estimate the current network load, and then select the appropriate Walsh code length and frame length. The simulation results show that the introduction of load estimation under medium and low load conditions can effectively reduce the resource occupation of the system and ensure that the performance of the random access protocol based on Walsh codes is not degraded. However, under high load conditions, a large resource overhead is still required to ensure the access performance of the system.

Author Contributions: Conceptualization, M.Y.; methodology, M.Y.; software, G.X.; validation, B.L.; formal analysis, G.X.; investigation, Y.Y.; resources, M.Y.; data curation, B.L.; writing—original draft preparation, G.X.; writing—review and editing, M.Y. and Y.S.; visualization, G.X.; supervision, B.L.; project administration, Y.Y.; funding acquisition, M.Y. All authors have read and agreed to the published version of the manuscript.

Funding: This research was funded by the National Natural Science Foundation of China under grant numbers 62071146 and 62171151 and the Fundamental Research Funds for the Central Universities (No. HIT.OCEF. 2021012).

Data Availability Statement: The data presented in this study are available on request from the corresponding author.

Conflicts of Interest: The authors declare no conflict of interest.

References

1. Dai, C.-Q.; Zhang, M.; Li, C.; Zhao, J.; Chen, Q. QoE-Aware Intelligent Satellite Constellation Design in Satellite Internet of Things. *IEEE Internet Things J.* **2021**, *8*, 4855–4867. [CrossRef]
2. Sanctis, M.D.; Cianca, E.; Araniti, G.; Bisio, I.; Prasad, R. Satellite Communications Supporting Internet of Remote Things. *IEEE Internet Things J.* **2016**, *3*, 113–123. [CrossRef]
3. Chen, Z.; Duan, X.; Wei, W.; Wang, S.; Ning, B.-J. Iridium-based nanomaterials for electrochemical water splitting. *Nano Energy* **2020**, *78*, 105270. [CrossRef]
4. Elbehiery, K.; Elbehiery, H. Cloud Technology: Conquest of Commercial Space Business. In *Internet of Things—Applications and Future*; Springer: Singapore, 2020; pp. 53–72.
5. Fu, X.; Su, Y. Performance Analysis of Satellite Internet of Things Access Protocol. In Proceedings of the International Conference in Communications, Signal Processing, and Systems, Adelaide, Australia, 14 December 2020; Springer: Singapore, 2020; pp. 1306–1311.
6. Kassas, Z.M. *Navigation from Low-Earth Orbit. Position, Navigation, and Timing Technologies in the 21st Century: Integrated Satellite Navigation, Sensor Systems, and Civil Applications*; IEEE: Piscataway, NJ, USA, 2021; pp. 1381–1412.
7. Bezgin, A.A.; Savochkin, A.A. Multiband Circular Polarization Antenna for Satellite System Argos-3 and GPS. In Proceedings of the 2019 Antennas Design and Measurement International Conference (ADMInC), St. Petersburg, Russia, 3 June 2019; pp. 30–32.
8. Del Rio Herrero, O.; De Gaudenzi, R. High Efficiency Satellite Multiple Access Scheme for Machine-to-Machine Communications. *Aerosp. Electron. Syst. IEEE Trans.* **2012**, *48*, 2961–2989. [CrossRef]
9. Liva, G. Graph-Based Analysis and Optimization of Contention Resolution Diversity Slotted ALOHA. *IEEE Trans. Commun.* **2011**, *59*, 477–487. [CrossRef]
10. Meloni, A.; Murroni, M.; Kissling, C.; Berioli, M. Sliding window-based Contention Resolution Diversity Slotted ALOHA. In Proceedings of the Global Communications Conference, Anaheim, CA, USA, 3–7 December 2012; pp. 3305–3310.
11. Lázaro, F. Decentralized Power Control for Slotted Spread Spectrum Aloha with Successive Interference Cancellation. In Proceedings of the International Itg Conference on Systems, VDE, Hamburg, Germany, 6–9 February 2017; pp. 1–6.
12. Bacco, F.M. Effcient M2M Communications via Random Access Satellite Channels. Doctor Dissertation, University of Siena, Siena, Italy, 2016; pp. 31–33.
13. Meloni, A.; Atzori, L. The Role of Satellite Communications in the Smart Grid. *IEEE Wirel. Commun.* **2017**, *24*, 50–56. [CrossRef]
14. Vassaki, S.; Pitsiladis, G.T.; Kourogiorgas, C.; Poulakis, M.; Panagopoulos, A.D.; Gardikis, G.; Costicoglou, S. Satellite-based sensor networks: M2M Sensor communications and connectivity analysis. In Proceedings of the International Conference on Telecommunications and Multimedia, Heraklion, Greece, 28–30 July 2014; pp. 132–137.
15. Bacco, M.; De Cola, T.; Giambene, G.; Gotta, A. TCP-Based M2M Traffic via Random-Access Satellite Links: Throughput Estimation. *IEEE Trans. Aerosp. Electron. Syst.* **2019**, *55*, 846–863. [CrossRef]
16. Elbert, B.R. *Introduction to Satellite Communication*; Artech house: Norwood, MA, USA, 2008.
17. Abramson, N. The Aloha System: Another alternative for computer communications. In Proceedings of the National Computer Conference, Atlantic City, NJ, USA, 1 January 1970; pp. 281–285.
18. Roberts, L.G. ALOHA packet system with and without slots and capture. *Acm Sigcomm Comput. Commun. Rev.* **1975**, *5*, 28–42. [CrossRef]
19. Choudhury Gagan, L.; Rappaport Stephen, S. Diversity ALOHA—A Random Access Scheme for Satellite Communications. *Commun. IEEE Trans.* **1983**, *31*, 450–457. [CrossRef]
20. Paolini, E.; Liva, G.; Amat, A.G.I. A structured irregular repetition slotted ALOHA scheme with low error floors. In Proceedings of the IEEE International Conference on Communications, Paris, France, 21–25 May 2017; pp. 1–6.
21. Graaf, P.W.D.; Lehnert, J.S. Performance comparison of a slotted ALOHA DS/SSMA network and a multi-channel narrowband slotted ALOHA network. In Proceedings of the Military Communications Conference, Fort Monmouth, NJ, USA, 2–5 October 1994; pp. 574–578.
22. Ma, G.; Ai, B.; Wang, F.; Zhong, Z. Joint Design of Coded Tandem Spreading Multiple Access and Coded Slotted ALOHA for Massive Machine-type Communications. *IEEE Trans. Ind. Inform.* **2018**, *14*, 4064–4071. [CrossRef]
23. Casini, E.; De Gaudenzi, R.; Herrero, O.D.R. Contention Resolution Diversity Slotted ALOHA (CRDSA): An Enhanced Random Access Schemefor Satellite Access Packet Networks. *IEEE Trans. Wirel. Commun.* **2007**, *6*, 1408–1419. [CrossRef]
24. Zhao, J.; Yue, X.; Kang, S.; Tang, W. Joint effects of imperfect CSI and SIC on NOMA based satellite-terrestrial systems. *IEEE Access* **2021**, *9*, 12545–12554. [CrossRef]
25. Shuai, H.; Guo, K.; An, K.; Zhu, S. NOMA-based integrated satellite terrestrial networks with relay selection and imperfect SIC. *IEEE Access* **2021**, *9*, 111346–111357. [CrossRef]
26. De Gaudenzi, R.; del Río Herrero, O.; Acar, G.; Barrabés, E.G. Asynchronous Contention Resolution Diversity ALOHA: Making CRDSA Truly Asynchronous. *Wirel. Commun. IEEE Trans.* **2014**, *13*, 6193–6206. [CrossRef]
27. Lee, D.; Lee, H.; Milstein, K.B. Direct sequence spread spectrum Walsh-QPSK modulation. *IEEE Trans. Commun.* **1998**, *46*, 1227–1232.
28. Zanella, A. Estimating Collision Set Size in Framed Slotted Aloha Wireless Networks and RFID Systems. *IEEE Commun. Lett.* **2012**, *16*, 300–303. [CrossRef]
29. Vogt, H. Multiple Object Identification with Passive RFID Tags. *Pervasive Comput.* **2002**, *3*, 98–113.

30. Cha, J.R.; Kim, J.H. Novel Anti-collision Algorithms for Fast Object Identification in RFID System. In Proceedings of the International Conference on Parallel and Distributed Systems-Workshops, 20–25 July 2005; pp. 63–67.
31. Wei, F.; Chen, W. Low Complexity Iterative Receiver Design for Sparse Code Multiple Access. *IEEE Trans. Commun.* **2017**, *65*, 621–634. [CrossRef]